Probing the homogeneous spectral function of a strongly interacting superfluid atomic Fermi gas in a trap using phase separation and momentum-resolved radio-frequency spectroscopy

Qijin Chen

Department of Physics and Zhejiang Institute of Modern Physics, Zhejiang University, Hangzhou, Zhejiang 310027, China

(Received 18 January 2011; published 29 July 2011)

It is of central importance to probe the *local* spectral function $A(\mathbf{k},\omega)$ of a strongly interacting Fermi gas in a trap. Momentum-resolved rf spectroscopy has been demonstrated to be able to probe the trap-averaged $A(\mathbf{k},\omega)$. However, the usefulness of this technique was limited by the trap inhomogeneity. Independent of a specific theory, here we propose that by studying the momentum-resolved rf spectra of the minority fermions of a phase-separated, population-imbalanced Fermi gas at low temperature, one can effectively extract $A(\mathbf{k},\omega)$ of a homogeneous superfluid Fermi gas (at the trap center). In support, we present calculated spectral functions and spectral intensity maps for various cases from BCS through Bose-Einstein condensation regimes using different theories.

DOI: 10.1103/PhysRevA.84.013624 PACS number(s): 67.85.−d, 03.75.Hh, 03.75.Ss, 74.20.−z

I. INTRODUCTION

Ultracold atomic Fermi gases has emerged as a rapidly developing field, bridging condensed-matter and atomic physics. Owing to their easy tunabilities such as the effective two-body interaction strength, population imbalance, and dimensionality, atomic Fermi gases can be viewed as a quantum simulator of many important condensed-matter systems, such as the Hubbard model and high-T_c superconductors [1,2].

Of central importance in a many-body system is the single-particle spectral function $A(\mathbf{k},\omega)$, especially in the strongly interacting regime (where different theories often do not agree); it can be used to calculate essentially all other physical quantities and to test various theories. For example, one important question, which has been long standing for high-T_c superconductors, is whether a pseudogap exists and how it evolves in the superfluid state. Because measurements often involve integration of the entire momentum space and the entire trap, the intrinsic spatial inhomogeneity introduced by the trapping potential constitutes a severe problem. It has been a long-sought goal to extract the *local or homogeneous* properties, especially $A(\mathbf{k},\omega)$, from measurements in the trap.

In this paper, we propose that one can use momentum-resolved rf spectroscopy in conjunction with a high population imbalance to measure the homogeneous spectral function $A(\mathbf{k},\omega)$ for the density and chemical potential at the trap center.

Since the first experimental realization of BCS–Bose-Einstein condensation (BEC) crossover, the most direct experimental probe of the single-particle properties is arguably the rf spectroscopy. The first generation of rf measurements involves integration over the entire trap and the whole momentum space [3], which led to a two-peak structure of the rf spectra at an intermediate temperature T below T_c. Due to the integrations, controversies arose regarding the origin of this two-peak structure. Tomographic rf spectroscopy [4] involves integration over the entire momentum space and therefore cannot be used to probe the spectral function. The recent Ho-Zhou scheme [5] allows one to calculate the density and fermionic chemical potential μ as a function of the radius r. However, it relies on the assumption of a *strict* harmonic trapping potential [6], often not satisfied. More importantly, it does not provide any microscopic information such as the spectral function.

The controversies regarding the origin of the aforementioned double peak structure have largely been cleared by the recent experiments [7] on ^{40}K using momentum-resolved rf spectroscopy. With momentum resolution, the rf spectroscopy essentially measures the centrally important $A(\mathbf{k},\omega)$, which is of central importance in a many-body system. However, this is true only for a *homogeneous* Fermi gas. The inherent spatial inhomogeneity severely limits the quantitative resolution of the extracted spectral function in the experiment of Ref. [7], which involves integration over the entire trap.

Here we address this inhomogeneity issue and show that it can be largely avoided utilizing phase separation at high population imbalances. In what follows we use two different theories to do computations. Despite some differences in *quantitative details*, we emphasize that *the validity of our proposal is model independent* and can be applied in other theories as well. Most importantly, *it is a proposal for experiment*.

As mentioned elsewhere [8], the use of ^{40}K rather than ^{6}Li is crucial in extracting $A(\mathbf{k},\omega)$, since there are no complications from final-state interactions [9] near the usual Feshbach resonance around 202 G. It is for this reason that the rf spectral intensity for ^{40}K is simply proportional to the spectral function $A(\mathbf{k},\omega)$. For ^{6}Li, extra efforts are needed in order to extract $A(\mathbf{k},\omega)$ from the rf spectral measurements.

The spectral function $A(\mathbf{k},\omega)$ can be used to uniquely construct the Green's function and the single-particle self-energy, for which different theories often give different results. Therefore, the more accurate the measurement of $A(\mathbf{k},\omega)$, the easier it is to test different theories. For example, different BCS-BEC crossover approaches [10,11] show different dispersive behavior of $A(\mathbf{k},\omega)$. The theoretical scheme used in Ref. [8] exhibits a clear downward dispersion in the spectral intensity map near T_c, manifesting an existing pseudogap before the onset of superfluidity at lower $T = T_c$, different from those [12,13] that follow the approach of Noziéres and Schmitt-Rink (NSR) [14]. A *quantitatively accurate* measurement of $A(\mathbf{k},\omega)$ should serve to unambiguously test these different schools of theories.

II. THEORETICAL FORMALISM

In a typical rf spectroscopy measurement, pairing takes place between two low-lying hyperfine states, which we refer to as levels 1 and 2. An rf field of frequency ν is used to excite the atoms in hyperfine level 2 to another hyperfine state, which is unoccupied initially and referred to as level 3. It has been shown previously [8] that for ^{40}K we have for the momentum-resolved RF current

$$I(\mathbf{k},\delta\nu) = \frac{1}{2\pi} A(\mathbf{k},\omega) f(\omega)\Big|_{\omega=\xi_{\mathbf{k}}-\delta\nu}, \tag{1}$$

where $A(\mathbf{k},\omega) = -2\,\mathrm{Im}\,G(\mathbf{k},\omega+i0)$ and $f(x)$ is the Fermi distribution function, with the transition matrix element set to unity. Here G is the Green's function of level 2 atoms, which we take to be the spin-down or minority species. Similar to angle-resolved photoemission spectroscopy in a usual condensed-matter system, the rf current measures $A(\mathbf{k},\omega)$ directly. Note that here $\delta\nu$ is the rf detuning. The frequency $\omega = \xi_{\mathbf{k}} - \delta\nu$ corresponds to the energy of level 2 atoms measured with respect to their Fermi level, where $\xi_{\mathbf{k}} = k^2/2m - \mu$ and μ is the chemical potential of atoms in level 2. We take $\hbar = 1$. It is obvious that when level 2 atoms are free, we have $\delta\nu = 0$ and $\omega = \xi_{\mathbf{k}}$; the former gives the sharp peak at zero detuning in previous rf spectra in Ref. [3], whereas the latter gives the free atom dispersion in the spectral intensity map in the ω-k plane in Ref. [7]. As has been used in the experiment [7], the angle-integrated "occupied spectral intensity" is given by $I^{\mathrm{photo}}(k,\omega) \equiv (k^2/2\pi^2)A(k,\omega)f(\omega)$.

The central issue here is to calculate the spectral function or equivalently the Green's function $G(K)$ for the minority (level 2) atoms. Here we present calculations using two different approaches. In the first, *pairing fluctuation*, approach, in the presence of population imbalance, detailed calculations of the superfluid phase diagram, the Green's function and density profiles in each phase can be found in Refs. [15] and [16]. In the case of phase separation in a trap, as shown in Fig. 2 of Ref. [15], there is a BCS superfluid core (without population imbalance), surrounded by the majority atoms, as confirmed experimentally [17,18]. To a first-order approximation, the density profile of the minority atoms can be obtained by truncating the density profile of an unimbalanced Fermi gas at the (sharp) phase separation boundary. With and without population imbalance, the normal state self-energy Σ_{pg} follows a rather simple BCS-like form [8,19]. In the superfluid state, the self-energy $\Sigma(K)$ contains two terms, associated with the condensed (Σ_{sc}) and noncondensed fermion pairs (Σ_{pg}), respectively: $\Sigma(\mathbf{k},\omega) = \Sigma_{pg}(\mathbf{k},\omega) + \Sigma_{sc}(\mathbf{k},\omega)$, where

$$\Sigma_{pg}(\mathbf{k},\omega) = \frac{\Delta_{pg}^2}{\omega+\xi_{\mathbf{k}}+i\gamma} - i\Sigma_0, \quad \Sigma_{sc}(\mathbf{k},\omega) = \frac{\Delta_{sc}^2}{\omega+\xi_{\mathbf{k}}}. \tag{2}$$

Here Δ_{pg}, Δ_{sc}, and $\Delta = \sqrt{\Delta_{sc}^2+\Delta_{pg}^2}$ are the pseudgogap, superfluid gap, and total excitation gap, respectively. The broadening $\gamma \neq 0$ and "incoherent" background contribution Σ_0 can be determined by fitting the experimentally measured rf spectra. The precise values of γ and Σ_0 and their T dependencies are not particularly important for the present purposes. Although the pseudogap contribution becomes less pronounced when the temperature is low enough to exhibit phase separation, it still makes a significant difference in comparison with a strict BCS theory.

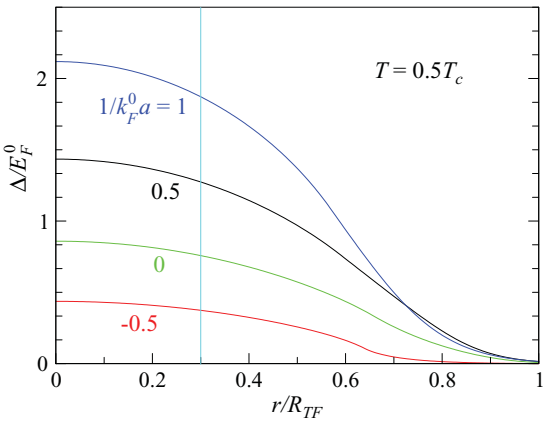

FIG. 1. (Color online) Radial profile of the excitation gap Δ/E_F^0 in the superfluid phase of a trapped Fermi gas without population imbalance for $1/k_F^0 a = -0.5$, 0, 0.5, and 1, corresponding to BCS through BEC regimes, calculated at $T = 0.5T_c$, using self-energy Eq. (2). The gap is nearly flat for $r < 0.3R_{TF}$.

In the second, *mean-field*, approach, as a test case, we use the same density profiles as obtained from the first approach, but take a simple broadened BCS self-energy,

$$\Sigma_{\mathrm{BCS}}(\mathbf{k},\omega) = \frac{\Delta^2}{\omega+\xi_{\mathbf{k}}+i\gamma} - i\Sigma_0. \tag{3}$$

Both approaches give the same form of quasiparticle dispersion $E_{\mathbf{k}} = \sqrt{\xi_{\mathbf{k}}^2+\Delta^2}$, albeit with different meanings of Δ. Obviously, they become equivalent above T_c, when we take $\gamma = \Sigma_0$. In contrast, they differ dramatically below T_c [19] because one contains a pseudogap while the other does not. In both approaches, γ and Σ_0 scale with local $E_F(r)$. As in Ref. [8], here we will take Σ_0 as T independent, γ linear in T/T_c, where T_c is calculated using the first approach. The rf spectra are finally convoluted with a Gaussian broadening function with a standard deviation σ, reflecting the instrumental resolution in experiment caused by, for example, finite energy and momentum resolution of both the rf pulse and the time-of-flight imaging technique.

III. RESULTS AND DISCUSSIONS

We first study the radial profile of the excitation gap in the superfluid phase. While throughout this paper we study each case in a harmonic trap with a local density approximation using both approaches, here we show in Fig. 1 the result from the *pairing fluctuation approach* [Eq. (2)]. It suffices to calculate for cases without population imbalance, since upon phase separation the superfluid core becomes unimbalanced so that the gap profile of minority atoms can be obtained by cutting off the curves in Fig. 1 at different radii for different population imbalances $p \equiv (N_\uparrow - N_\downarrow)/(N_\uparrow + N_\downarrow)$. For simplicity, here the data were all calculated at $T = 0.5T_c$, below which phase separation takes place at unitarity [15]. The curves, as labeled, correspond to $1/k_F^0 a = -0.5$ (BCS case), 0 (unitary), 0.5 (pseudogap), and 1.0 (BEC) cases, respectively, where a is the interfermion s-wave scattering

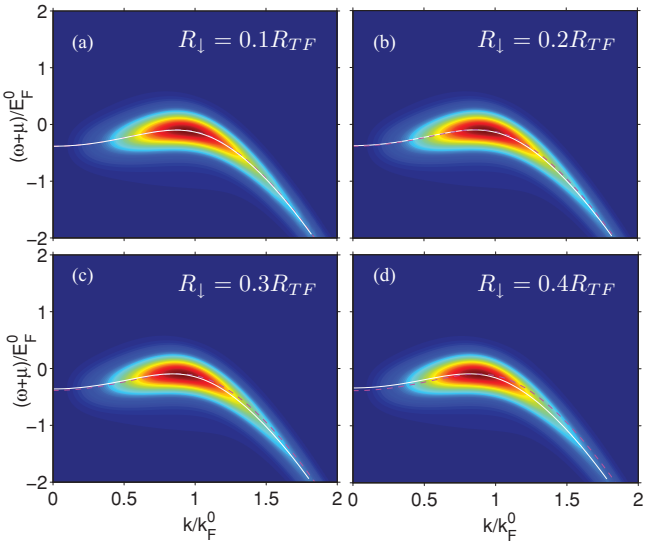

FIG. 2. (Color online) Occupied spectral intensity maps $I^{\rm photo}(k,\omega)$ for the minority atoms of a population-imbalanced, phase-separated unitary Fermi gas in a harmonic trap for (a) $R_\downarrow = 0.1R_{TF}$, (b) $0.2R_{TF}$, (c) $0.3R_{TF}$, and (d) $0.4R_{TF}$, respectively, calculated at $T = 0.13T_F^0$, using self-energy Eq. (2). The (magenta) dashed curves represent the local (or homogeneous) dispersion at the trap center, and the (white) solid curves are the quasiparticle dispersion given by the loci of the peak location of the EDC. The broadening parameters $\Sigma_0 = \gamma(T_c) = 0.1E_F^0$ at the trap center. Here the spectral intensity increases from 0 (dark blue) continuously through the maximum (dark red). The quantitative scale for, for example, panel (c) may be seen from Fig. 4. For the instrumental Gaussian broadening, we take $\sigma = 0.2E_F^0$ (as extracted [8] from the experiment in Ref. [7]). Up to $R_\downarrow = 0.4R_{TF}$, the two sets of curves are essentially indistinguishable.

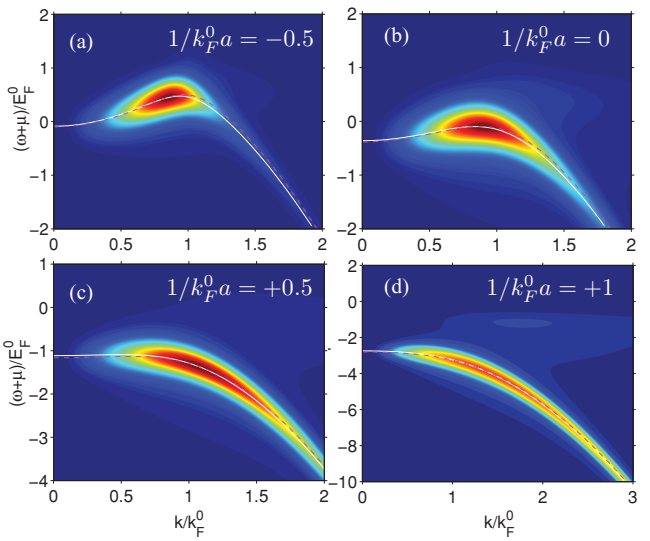

FIG. 3. (Color online) Occupied spectral intensity maps $I^{\rm photo}(k,\omega)$ for the minority atoms of a population-imbalanced, phase-separated Fermi gas with $R_\downarrow = 0.3R_{TF}$ for (a) $1/k_F^0a = -0.5$ (BCS case), (b) 0 (unitary), (c) 0.5 (pseudogap), and (d) 1.0 (BEC case), calculated at $T = 0.09T_F^0$, $0.13T_F^0$, $0.15T_F^0$, and $0.15T_F^0$, respectively, *assuming self-energy* Eq. (3). The legends are the same as in Fig. 2. The parameters $\Sigma_0 = \gamma(T_c)$ at the trap center are (a) $0.1E_F^0$, (b), (c) $0.2E_F^0$, and (d) $0.35E_F^0$. T_c is taken from the pairing fluctuation approach. The instrumental broadening $\sigma = 0.2E_F^0$. For all cases, the two sets of curves are essentially indistinguishable.

length, $E_F^0 \equiv k_B T_F^0 \equiv \hbar^2(k_F^0)^2/2m$ and k_F^0 are the global Fermi energy and Fermi momentum in the noninteracting limit for the majority atoms, respectively. Figure 1 reveals that for $r < 0.3R_{TF}$, the gap is nearly flat from BCS through BEC regimes, where R_{TF} is the Thomas-Fermi radius. Since the pseudogap increases with pairing strength and it is already comparable with the zero T gap at unitarity [2,7], the *total* gap profile $\Delta(r)$ remains nearly flat for small r even at higher $T \approx T_c$ at unitarity and in the BEC regime [20].

With this knowledge, now we study the occupied spectral intensity maps of the minority (spin-down) atoms in the $[\omega + \mu(r)]$–k plane for different degrees of population imbalance p, as characterized by the radius $R_\downarrow$ of the minority atomic gas. For illustration purpose, we present the result from the *pairing fluctuation approach* Eq. (2) for the unitary case with phase separation in Fig. 2, for different $R_\downarrow$. Note here that, as in Ref. [8], we use $\omega + \mu(r)$ instead of ω in the vertical axis, since the former combination is independent of r representing the single-particle energy measured from the bottom of the band. While Fig. 2(a) corresponds to an extremely high population imbalance, which may not be readily realizable in experiment, Figs. 2(c) and 2(d) are certainly accessible experimentally [17]. For example, for ^{6}Li, Ref. [18] reports a phase-separation boundary at about $0.3R_{TF}$ at $p = 0.54$. The (magenta) dashed curves represent the local (or homogeneous) dispersion at the trap center, and the (white) solid curves are the quasiparticle dispersion given by the loci of the peak location of the energy distribution curves (EDCs). It is evident that up to $R_\downarrow = 0.4R_{TF}$, the two sets of curves are essentially indistinguishable.

Shown in Fig. 3 are the occupied spectral intensity maps of the minority atoms of population-imbalanced, phase-separated atomic Fermi gases in a harmonic trap with minority radius $R_\downarrow = 0.3R_{TF}$ for different pairing strength from BCS through BEC. Here we show the results calculated using the *mean-field* self-energy Eq. (2). Since the atomic cloud shrinks with increasing $1/k_F^0a$, these same $R_\downarrow$ correspond to an imbalance of about $p = 0.9$–0.7. Here the parameters γ and Σ_0 increase from BCS to BEC, reflecting an increasing excitation gap. Clearly, for all cases shown, the dispersions extracted from the trap averaged minority atoms are very close to that calculated at the trap center.

Note that the upward dispersing branch of thermally excited quasiparticles is completely suppressed by $f(\omega)$ and becomes invisible here. However, its leftover at large k form a very weak broad peak at negative ω, as indicated by the light blue area above the downward dispersing branch. At higher T, this feature [21] naturally explains the artificial abrupt jump in the quasiparticle dispersions extracted at higher T using a *single peak fit* in Fig. 1 of Ref. [22].

Finally, shown in Fig. 4 is a direct comparison of the (occupied) spectral function between the atoms at the trap center (black solid and red dashed curves) and the trap averaged minority atoms (green long-dashed and blue dot-dashed curves) of a highly population-imbalanced, phase-separated Fermi gas, from the pairing fluctuation approach. The curves

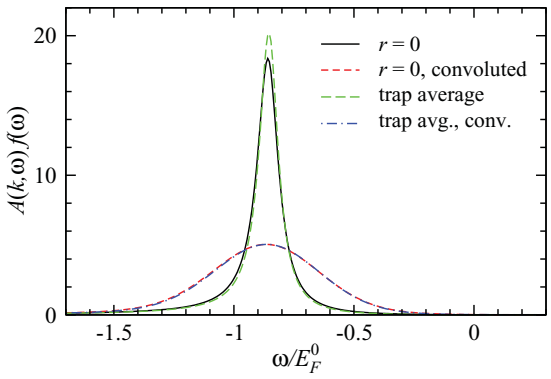

FIG. 4. (Color online) Comparison of occupied spectral function $A(k,\omega)f(\omega)$ between atoms at the trap center (black solid and red dashed curves) and trap averaged minority atoms (green long-dashed and blue dot-dashed curves) for a population-imbalanced, phase-separated unitary Fermi gas with $R_\downarrow = 0.3R_{TF}$ at $T = 0.5T_c = 0.13T_F^0$. The spectra are calculated for $k = 0.88k_F^0 \approx \sqrt{2m\mu(r=0)}$ near the Fermi surface, using self-energy Eq. (2). The narrow peaks are the intrinsic spectral line, whereas the broad ones are those convoluted with an instrumental broadening function. The broadening parameters Σ_0, γ, and σ are the same as in Fig. 1. The trap averaged minority spectral function is nearly the same as that at the trap center.

are for $k = 0.88k_F^0 \approx \sqrt{2m\mu(r=0)}$, which is near the Fermi level [where $A(k,\omega)$ is most sensitive to the variation of Δ] at the trap center. The spectral peaks at $+E_{\mathbf{k}} \approx \Delta$ are suppressed by $f(\omega)$. The narrow peaks are the spectral lines without instrumental broadening, and the broad ones are the same result but with instrumental broadening. There are small differences between the unconvoluted spectral peaks (black solid) and (green long-dashed curves) in the peak location and peak height (or equivalently peak width). This is primarily due to the gradually decreasing broadening parameters caused by decreasing local $E_F(r)$ as r increases, leading to slightly higher peak and smaller average gap (given by the peak location). We emphasize that these differences are barely discernible and are completely washed out by instrumental broadening, as revealed by the complete overlap between the two broad peaks. The complete spectral function $A(k,\omega)$ can be obtained by dividing the unconvoluted lines by $f(\omega)$.

Indeed, a comparison between Fig. 2(c) and Fig. 3(b) reveals that the spectral lines from self-energy Eq. (3) have a broader background than that from Eq. (2). Precise spectral function measurement as shown in Fig. 4 is expected to tell them apart.

IV. CONCLUSIONS

In conclusion, in the presence of phase separation for a highly population-imbalanced, strongly interacting Fermi gas, the trap averaged quasiparticle dispersion of the minority atoms is very close to that at the trap center. Therefore, one can use the former dispersion to extract effectively not only the excitation gap and the fermionic chemical potential but also the *centrally important* spectral function at the trap center. This scheme does not depend on our particular BCS-BEC crossover theory, nor does it depend on the strict harmonicity of the trapping potential. For higher T or deeper BEC regime where phase separation is prohibited, one may use an rf pulse with a narrow cross section (as has been reported experimentally [23]) *without* population imbalance to achieve similar results. In this way, the narrow rf beam mimics the effect of *artificial* phase separation by picking up signals only from the central part of the trap [24].

ACKNOWLEDGMENTS

This work is supported by NSF of China (Grant No. 10974173), the 973 Program of China (Grant No. 2011CB921300), Fundamental Research Funds for Central Universities of China (Program No. 2010QNA3026), PCSIRT (Contract No. IRT0754), Changjiang Scholars Program of the Ministry of Education of China, Qianjiang RenCai Program of Zhejiang Province (No. 2011R10052), and Zhejiang University (Grant No. 2009QNA3015).

[1] A. J. Leggett, Nat. Phys. **2**, 134 (2006).
[2] Q. J. Chen, J. Stajic, S. N. Tan, and K. Levin, Phys. Rep. **412**, 1 (2005).
[3] C. Chin, M. Bartenstein, A. Altmeyer, S. Riedl, S. Jochim, J. Hecker-Denschlag, and R. Grimm, Science **305**, 1128 (2004).
[4] Y. Shin, C. H. Schunck, A. Schirotzek, and W. Ketterle, Phys. Rev. Lett. **99**, 090403 (2007).
[5] T.-L. Ho and Q. Zhou, Nat. Phys. **6**, 131 (2009).
[6] Confirmed by T.-L. Ho (private communications).
[7] J. T. Stewart, J. P. Gaebler, and D. S. Jin, Nature (London) **454**, 744 (2008).
[8] Q. J. Chen and K. Levin, Phys. Rev. Lett. **102**, 190402 (2009).
[9] S. Basu and E. J. Mueller, Phys. Rev. Lett. **101**, 060405 (2008); Y. He, C.-C. Chien, Q. J. Chen, and K. Levin, *ibid.* **102**, 020402 (2009); A. Perali, P. Pieri, and G. C. Strinati, *ibid.* **100**, 010402 (2008); M. Punk and W. Zwerger, *ibid.* **99**, 170404 (2007); Z. Yu and G. Baym, Phys. Rev. A **73**, 063601 (2006).
[10] K. Levin, Q. J. Chen, Y. He, and C.-C. Chien, Ann. Phys. **325**, 233 (2010); Q. J. Chen, Y. He, C.-C. Chien, and K. Levin, Rep. Prog. Phys. **72**, 122501 (2009).
[11] S.-Q. Su, D. E. Sheehy, J. Moreno, and M. Jarrell, Phys. Rev. A **81**, 051604(R) (2010).
[12] A. Perali, P. Pieri, G. C. Strinati, and C. Castellani, Phys. Rev. B **66**, 024510 (2002).
[13] P. Massignan, G. M. Bruun, and H. T. C. Stoof, Phys. Rev. A **77**, 031601(R) (2008).
[14] P. Nozières and S. Schmitt-Rink, J. Low Temp. Phys. **59**, 195 (1985).
[15] C.-C. Chien, Q. J. Chen, Y. He, and K. Levin, Phys. Rev. Lett. **98**, 110404 (2007).

[16] Y. He, C.-C. Chien, Q. J. Chen, and K. Levin, Phys. Rev. A **75**, 021602(R) (2007); Phys. Rev. B **76**, 224516 (2007).

[17] G. B. Partridge, W. H. Li, R. I. Kamar, Y. A. Liao, and R. G. Hulet, Science **311**, 503 (2006); M. W. Zwierlein, A. Schirotzek, C. H. Schunck, and W. Ketterle, *ibid.* **311**, 492 (2006).

[18] Y. Shin, C. H. Schunck, A. Schirotzek, and W. Ketterle, Nature (London) **451**, 689 (2008).

[19] Q. J. Chen, K. Levin, and I. Kosztin, Phys. Rev. B **63**, 184519 (2001).

[20] In the BEC regime, the gas cloud shrinks so that phase separation boundary also moves torward the trap center.

[21] Q. J. Chen, APS March Meeting, 2009 [http://meetings.aps.org/link/BAPS.2009.MAR. A16.5].

[22] J. P. Gaebler, J. T. Stewart, T. E. Drake, D. S. Jin, A. Perali, P. Pieri, and G. C. Strinati, Nat. Phys. **6**, 569 (2010).

[23] T. Drake *et al.*, APS March Meeting, 2011 [http://meetings.aps.org/link/BAPS.2011.MAR.P45.3].

[24] It should be noted that the boundary of a focused rf pulse may not be as sharp as the interface of phase separation, making our phase-separation method a better choice at low T.